Experimental Method to Find the Flux Variation on the Receiver of Central Receiver System

Mahesh P. Kumbhare[1], Ganesh E. Kondhalkar[1], Kashinath H. Munde[1], Vikaskumar K. Mehtre[1]

[1]Department of Mechanical Engineering, Anantrao Pawar College of Engineering & Research, Parvati, Pune (MH)

Article Info
Page Number:479-490
Publication Issue:
Vol 71 No. 1 (2022)

Article History
Article Received*: 02 February 2022*
Revised*: 10 March 2022*
Accepted*: 25 March 2022*
Publication*: 15 April 2022*

Abstract

Abstract: Concentrating solar technologies can be used for power generation as well as industrial process heating. A point focusing solar collector forms a flux distribution on the receiver plate in two dimensions at the focal plane. A tool or method for analyzing the flux distribution nature can be great helpful to know the optical quality of the receiver. Experiments needs to be carried out in the focal region of the concentrating collector to know the flux distribution on the receiver plate. Behavior of the flux distribution are measured by flux mapping techniques and also these methods can provide accurate results, but the equipment of this method is specialized and costly. A simple method need to estimate the optical quality like flux distribution and focus size for central receiver system. Thermocouple method is used for finding the distribution of flux density on the receiver. This information is helpful in the design of the receiver size, shape and the choice of the material.

Keywords- Heliostat, Flux distribution, Area Element.

1.0 INTRODUCTION

In a solar central receiver system, solar radiation is concentrated on a tower-mounted heat exchanger (Receiver) by the use of mirrors called heliostats. In this system all the heliostat focus at the center of receiver that cause point focus at the center of receiver. The flux distribution on the receiver is main term which is related to energy generation form the solar central receiver system. A point focusing on the central receiver form a flux distribution in two dimension (X, Y) at the focal plane.

The flux measurement techniques can be classified in indirect and direct measurement. Charged Coupled Devices (CCD) cameras are used in indirect method to measure the solar radiation reflected off a surface (Elsayed, Fathalah and Rabghi 1995). A flux sensor which directly gives a measurement signal proportional to the irradiative flux is used in direct measurement method. Calorimeter method which is indirect method is used for small-scale heliostat field to determine the flux distribution. (holger Kretzschmar (2007).

The equipment's are specialized and costly. A simple and indirect optical characterization method called focus test has therefore been proposed by Sharma (2005).It is based on temperature measurement in the focal plane of the solar dish concentrator and hence to estimate the flux concentrated. This test is used to find out characteristics like focus size, total input solar power and local concentration ratio of the dish concentrator. Sharma et al. (2005) having implemented this procedure on a paraboloidal type of dish concentrator, called ARUN 160 (kedare et al., 2006). Same test procedure used for optical characterization are reported for scheffler dish concentrator and for more accuracy measuring the temperature at a large number of point on the receiver plate

(V.P. Muley, 2010). Two approaches are used (1) isotherm method and (2) area element method, for analyzing the temperature distribution on focus plate.

In this paper, the flux distribution on the receiver is experimentally carried for solar central receiver system by implementing the thermocouple method proposed by Sharma (2005) and Muley (2010). Flux distribution is the temperature profile on the receiver at desired focal region of concentrators. Form this temperature profile flux can be calculated and form the whole flux value on the receiver flux distribution will be find out. The estimation of temperature distribution on the receiver plate is carried out more rigorously by measuring temperature at a large number of points on the receiver plate by using area element method. The mathematical formulation for the the experimental method, test procedure and its result are discussed in this paper.

2.0 MATHEMATICAL FORMULATION FOR EXPERIMENTAL METHOD

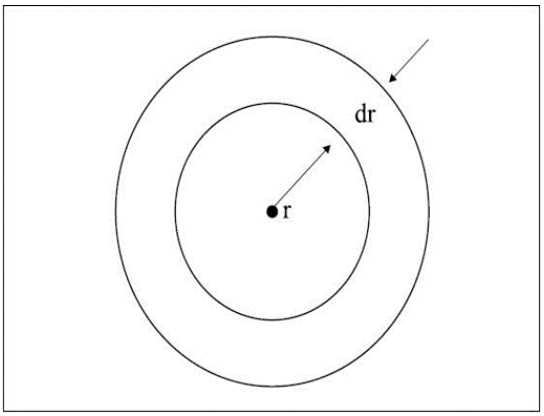

Fig. 1 A typical strip on Receiver plate

A thin (1mm) flat copper plate with known thermal conductivity is placed in front of the heliostats (mirror). Solar rays reflected from the mirror would be concentrated on the receiver plate. Energy balance equation for receiver plate exposed to reflected radiation is given below.

Consider a small strip of radius ‘r’ and width ‘dr’ as shown in fig. 1. The energy balance equation for this small strip, can be expressed as

Absorbed energy = Energy loss by conduction + Energy loss by convection + Energy loss by radiation

Here conduction loss consists of two parts, heat conduction from one area element to the neighboring area element and the heat conduction through insulation provided on the back side of receiver plate. Sharma et al. (2005), suggested that the heat loss due to conduction from a strip to neighboring strips is negligible as compared to convection and radiation losses. This is valid only when the thickness of the plate is less and the convective and radiation components are of very high magnitude than the conduction term. Sharma et al. (2005) assumed that the convective heat transfer coefficient and radiation losses are same for both sides of the plate. The above equation is written as

$$(2\pi r)dr\Phi_c(r)\alpha = dq_r - dq_{(r+dr)} + [h(T_r - T_{amb}) + \sigma\varepsilon(T_r^4 - T_{sky}^4)](2\pi r)dr + $$

(1)

The above equation is reduced as follows,

$$\Phi_c(r)\alpha + (k * t)\frac{d^2t}{dr^2} = h(T_r - T_{amb}) + \sigma\varepsilon\left(T_r^4 - T_{sky}^4\right) + \frac{k_i}{L}(T_r - T_{amb})$$

(2)

The thermal conductivity of copper plate is 385 W/m^2 and the plate thickness is about 1 mm, thus $(k * t)$is 0.0385 W/K. The measured temperature profile suggested that the maximum value of $\frac{d^2t}{dr^2}$is of the order of 0.31 K/m^2. So $(k * t)$ $(\frac{d^2t}{dr^2})$ is about 0.12 W/m2. It is quite small compared to the convective and radiation loss terms of Equation 1, which are of the order of 257.92 W/m^2 and 38.95 W/m^2 respectively. Hence in Equation 2, (k *t) $(\frac{d^2t}{dr^2})$ term can be neglected [3]. As more number of heliostats will be used the temperature obtained at the focus would be high and more uniform, also considering finer grids of thermocouple there would be significant decrease in the value of the term $(k * t)$ $(\frac{d^2t}{dr^2})$, hence this term can be neglected. In the experimental setup the receiver plate is covered by ceramic insulation to suppress the convection and radiation losses from back side of plate. So the final energy balance equation will be as follows-

$$\Phi_c(x) = \frac{[h(T_x - T_{amb}) + \sigma\varepsilon\left(T_x^4 - T_{sky}^4\right) + (\frac{k_i}{L})(T_x - T_{amb})]}{\alpha}$$

(3)

Where, $\Phi_c(x)$ is the solar flux at a distance 'x' from the center of the focus, W/m^2.

h- Convective heat transfer coefficient of the focus plate, W/m^2

T_x - temperature of the area element at radius 'x' from the center of the focus, K

T_{amb} - ambient temperature, K

Tsky - (T_{amb} - 6) ,K

K_i - thermal conductivity of the insulation, W/m-K

L- Thickness of the insulation layer, m

σ - Stefan-Boltzmann constant, W/m^{2}K^4

ϵ -emissivity of the plate

α - absorptance of the plate for solar radiation

The convective heat transfer coefficient of the plate can be calculated from the following correlation,

h=5.7+3.8×v(10) (4)

Where,

v - Air velocity m/s

Flux can easily calculated with the help of equation (3) and gives the idea of flux distribution on the receiver plate.

3.0 THERMOCOUPLE METHOD

For finding the flux distribution form the temperature profile which is generated at the receiver plate thermocouple method is used. The temperature profile measure with the help of k type thermocouples. For proper measurement of temperature distribution, thermocouples are arrange in an array at the even distance on the receiver plate. For the thermocouple arrangement, area element method is used. In this method, each thermocouple is assumed to represent the temperature of a finite area element of h1 X v1 which is 200mm X 200mm as shown in Fig. 2. It is assumed that the thermocouple represents the average temperature of the respective area element. The average temperature of the receiver plate is calculated based on the values of all temperature points. The convective and radiative losses are then calculated for all area elements for all temperatures points. It may be mentioned that each thermocouple is assumed to be representing same amount of area.

Here two cases of heliostats sizes are taken for experimentation purpose. In 1st case 4 Heliostats of 2ft X 2ft size and in 2nd case 4 heliostats of 3ft X 3ft size are used for experimentation. A thermocouple represent the temperature of square area of size 0.6m × 0.6m for 1st case and 0.8m × 0.8m for 2ndcase. The area of the focus plate, lying outside the area covered by the thermocouple grid, is neglected.

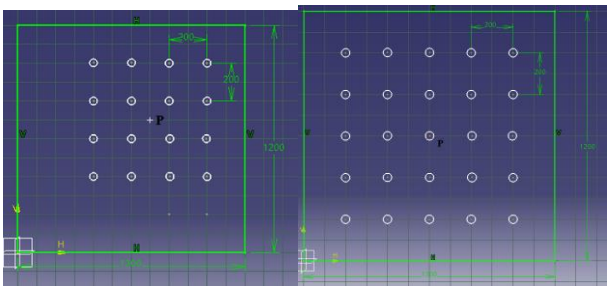

(a) **(b)**

Fig. 2 (a) 16 Thermocouple grid with 0.6m × 0.6m area and (b) 25 Thermocouple grid with 0.8m × 0.8m area.

The heliostats are rectangular in size, hence the receiver is also taken as rectangular of size 1.2m X1.2m for accommodating all the flux falling on the receiver without any spillage.

4.0EXPERIMENTAL SET – UP

The experimental set-up consists of mainly heliostat array and a receiver plate with thermocouple grid and insulation sheet.

4.1 Receiver plate and Insulation thickness

In this experimental setup to have fast heat conduction a copper plate is used as a receiver plate and to have the fast response time the thickness of the receiver plate is taken as 1mm.The set-up

consists of a metal plate (material: copper, 1.2m X 1.2m, thickness 1mm) and is referred as focus plate. The focus plate was mounted at 6 meter from the heliostats. The arrangements were done such that the receiver received all the reflected rays from the concentrators. For the two cases of heliostats as discussed earlier 16 and 25 thermocouples are fixed in a grid of 4×4 and 5×5 respectively; with distance between two thermocouples is 200mm, the thermocouple grid thus cover an area of 0.6 m × 0.6 m and 0.8m × 0.8m respectively. Each thermocouple indicates the average temperature of grid area of 0.2m × 0.2m. The thermocouples were brazed to the focus plate from back side. A layer of ceramic wool insulation of thickness 25mm is provided over the thermocouples to minimize the heat losses. Mild steel plate was used to clamp and hold the insulation as shown in figure 4. Figure 3 shows the arrangement of thermocouples on the receiver plate.

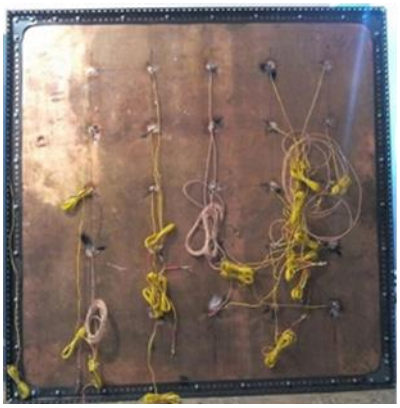

Fig.3 Arrangement of thermocouples on back side of receiver plate.

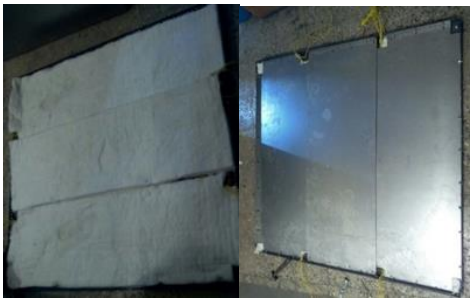

Fig. 4 Insulated back side of receiver plate

4.2 Heliostat system

Generally a conventional heliostat is mounted on a pedestal and is pivotally rotatable about altitudinal and azimuthal axes. Each axis is equipped with a motorized limb that can pivotally rotate the mirror of the heliostat to adjust its position. Thus in conventional system for a single heliostat 2 motors are required and the size of the motor changes with the size of the heliostat. In the presented system, a number of heliostats are mechanically oriented and linked on a rotatable shaft. The advantage of this linked mechanism on a rotatable shaft is that all the heliostats can be controlled by a single DC motor and actuator arm. This helps in significantly cutting the cost of motors used in conventional system. Following are the figures of heliostat:

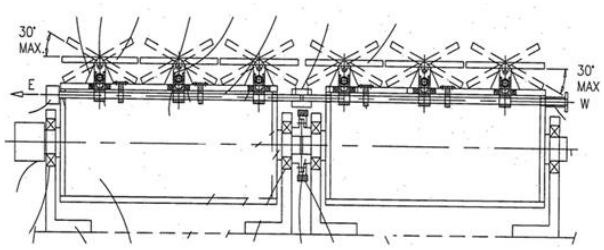

Fig. 5 schematic diagram of mechanically linked heliostat

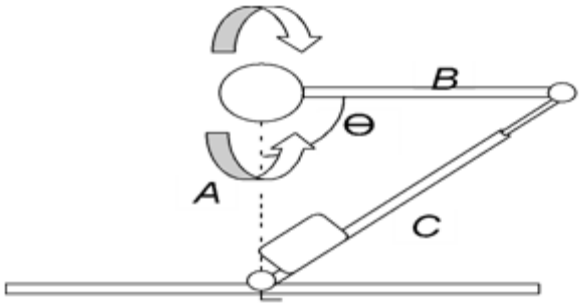

Fig.6 Actuator mechanism to control the elevation motion of the heliostat

All the mirrors are mounted on a single shaft, the shaft is given motion using DC motor, this DC motors tracks the azimuthal motion of the sun while the actuator mechanism as shown in figure 5 and 6, helps in tracking the elevation motion of the sun. An arrangement of heliostat array and receiver plate are shown in figure 7 and the figure 8 shows the experimental setup.

Fig. 7 Heliostat array (left); image on the focus plate (right).

Fig. 8 Experimental setup

4.3 Testing Procedure

The receiver plate with the thermoxouples is mounted at the desired place(in front of heliostat array) and heliostats are focused onto it.The thermocouple readings and the air temperature readinds are logged onto a computer by using data acquisition sysytem (eScan). Digital wind anemometer is used to measure the wind speed. The heliostat system is focused manually at the starting time and after that its automatic tracking mechanism takes over for continuous tracking during the whole testing period. The radiation data (global and diffuse) are recorded by using radiation pyranometers which is connected to the data logger.

For 1st case (2ft X2ft heliostats) 16 thermocouples temparature are reacorded at evergy 10 sec throuth out the testing period.

This experiment is carried out around the solar noon and measurment of temparature are made when temperature receods show the steady state value for about 10 minuts since trhe time constant of focus plate is estimated to be 6 minutes.Wind speed and solar radiation are measured at every 10 minuts.

In simillarly manner above test procedure is carried out to the 2nd case (3ft X 3ft heliostats) receiver having 25 thermocouples.

The experiment are carried out on 28th, 29th, 30th, 31st May 2016 for 1st case and on 9, 15, 16 June 2016 for 2nd case.

5.RESULTS AND DISCUSSION

Based on the temprature records of the receiver plate, the flux distribution on the receiver plate are estimated by using area element method.Following are the flux and temparature of the all area elements,

Case-1: For 2feet × 2feet heliostat and receiver with 16 thermocouple.

Table 1 Observation Table: 29th May, 13:00 hrs

Thermocouple	radius from centre (m)	temperature (k)	conductive	convective	radiative	Flux (W/ m^2)
T1	0.424	344.36	198.53	550.09	28.49	1036.14
T2	0.316	352.54	237.79	658.88	34.77	1241.93
T3	0.316	335.7	156.96	434.91	22.31	818.91
T4	0.424	326.23	111.50	308.96	16.08	582.06
T5	0.316	353.84	244.03	676.17	35.81	1274.69
T6	0.141	345.24	202.75	561.79	29.15	1058.25
T7	0.141	338.06	168.29	466.30	23.95	878.05
T8	0.316	325.4	107.52	297.92	15.56	561.34
T9	-0.316	337.54	165.79	459.38	23.59	865.01
T10	-0.141	334.79	152.59	422.81	21.69	796.12
T11	-0.141	317.1	67.68	187.53	10.57	354.37
T12	-0.361	323.69	99.31	275.18	14.50	518.65
T13	-0.424	325.57	108.34	300.18	15.67	565.58
T14	-0.361	323.87	100.18	277.57	14.61	523.15

T15	-0.361	322.23	92.30	255.76	13.61	482.23
T16	-0.424	318.13	72.62	201.23	11.17	380.03
			Average flux	746.03		

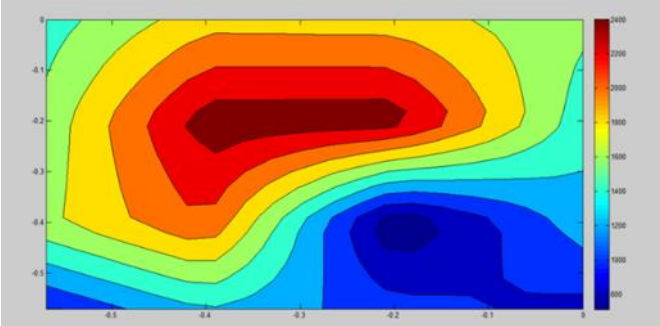

Fig.9 Flux distribution of 4 heliostat (2feet × 2feet) on the Receiver Using MATLAb Software (29 may at 1300Hrs)

Case-2: For 3feet × 3feet heliostat and receiver with 25 thermocouple.

Table 2 Observation Table: 16 June, 1120 hrs.

Thermocouple	radius from centre (m)	temperature (k)	conductive	convective	radiative	Flux (W/ m^2)
T1	0.565	334.94	153.31	424.802	21.79	799.88
T2	0.447	367.33	308.78	855.589	47.29	1615.55
T3	0.4	369.43	318.86	883.519	49.20	1668.77
T4	0.447	336.98	163.10	451.934	23.20	850.98
T5	0.565	320.89	85.87	237.937	12.80	448.81
T6	0.447	353.1	240.48	666.33	35.22	1256.04
T7	0.282	403.4	481.92	1335.32	84.83	2536.09
T8	0.2	395	441.60	1223.6	75.13	2320.44
T9	0.282	358.55	266.64	738.815	39.67	1393.50
T10	0.447	329.32	126.34	350.056	18.06	659.27
T11	0.4	383.4	385.92	1069.32	62.72	2023.94
T12	0.2	411.6	521.28	1444.38	94.90	2747.41
T13	0	373.67	339.22	939.911	53.14	1776.36
T14	-0.2	352.35	236.88	656.355	34.62	1237.14
T15	-0.4	323.66	99.17	274.778	14.48	517.91
T16	-0.447	396	446.40	1236.9	76.25	2346.07
T17	-0.282	400	465.60	1290.1	80.83	2448.70
T18	-0.2	358.31	265.49	735.623	39.47	1387.45
T19	-0.282	338.92	172.42	477.736	24.56	899.61
T20	-0.447	377.3	356.64	988.19	56.63	1868.61
T21	-0.565	354.17	245.62	680.561	36.08	1283.01
T22	-0.447	365.38	299.42	829.654	45.55	1566.17
T23	-0.4	340.57	180.34	499.681	25.73	941.00
T24	-0.447	332.1	139.68	387.03	19.88	728.79
T25	-0.565	315.89	61.87	171.437	9.87	324.24

			Average flux	1425.83

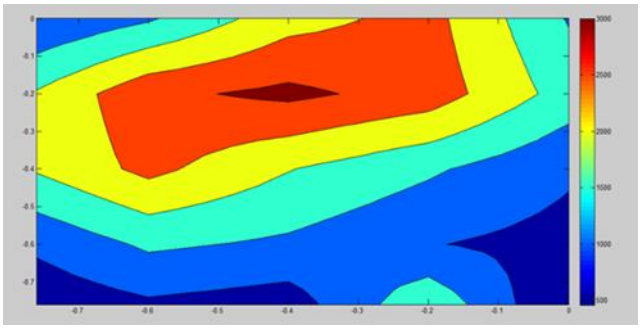

Fig.10 Flux distribution of 4 heliostat (3feet × 3feet) on the Receiver Using MATLAb Software (16 June at 1120Hrs).

From the above temperature table, the average temperature of the receiver plate for case1 was calculated using the area weighted method and was found to be 332.77k and peak temperature is 353.84k. Simillarly the average temperature of the receiver plate for case2 was calculated using the area weighted method and was found to be 345.9 k and peak temparature is 411.60k. This temperature is higher than the 1st case average temperature. It show that as heliostat size increases temperature of plate and heat flux losses is also increases.

From the above images, we see that nature of flux distribution image obtained using matlab and experimental flux value at different times at different days. For both cases it is clear that experimental flux concentration is more at the centre, but in case1 flux distribution is more concerted at the centre as compare the case2. Also in case1 flux distribution is not even as compare to the case2, in case2 flux distribution drop is less and in case1 flux distribution drop is more. The above image shows that the more concentration of the flux at the center of receiver plate tends to more heat losses.

ACKNOWLEDGEMENT

We would like to express our sincere gratitude to Dr. Pradeep J. Awasare (Adjunct Professor), Er. Sudarshan Natu (Innovation Club Member) for their invaluable guidance and support throughout the research process. We also wish to thank Dr. Sunil B. Thakare (Principal, APCOER, Pune) for their support. Finally, we are grateful to all of the research participants who generously gave their time and effort to this project.

6 CONCLUSION

Receiver size is the main parameter for designing and it also affect the power loss and cost of the system. Mainly size of the receiver is depened on the optical regeion of flux(flux disribution area).For determinng the flux distribution the above experimenat method are used and from this method the flux value are calculated. Also it provides the size of the focus, the total incident power and concentration ratio.

Table 3 Flux values of both Case.

Case No.	Day	Time(Hrs)	Peak Flux W/m^2	Average Flux W/m^2
1	29-05-2016	13:00	1274.69	746.0.3
2	16-16-2016	11:20	2747.41	1425.83

Form the above flux value it is concluded that using this experimental method proper flux distribution is find out. In case 2 flux distribution is more even and high flux value as compare to case 1. Also from the above table and flux distribution images it is clear that focus size and flux.Distribution increase according to the increment in the size of heliostat.

7. ACKNOWLEDGMENT

The authors would like to thank Dr. Ravindra Patwardhan sir and Mr. Akole sir for providing the research facility.

REFERENCES

[1] Moustafa M. Elsayed, Kadry A. Fathalah and Omar M. Al- Rabghi, 'Measurements of solar flux density distribution due to a flat heliostat', Solar energy, vol 54, 403 – 411 (1995).
[2] Blackmon J.B.,"Development and performance of digital image radiometer for heliostat evaluation at solar one",Journal of solar Energy Engineering,107,315-321(1985).
[3] V. Rakesh Sharma, S.B. Kedare, 'A simple method to determine optical quality of Paraboloid concentrating solar thermal collector', 2006.
[4] Dhabliya, M. D. (2018). A Scientific Approach and Data Analysis of Chemicals used in Packed Juices. Forest Chemicals Review, 01–05.
[5] Dhabliya, D. (2021a). AODV Routing Protocol Implementation: Implications for Cybersecurity. In Intelligent and Reliable Engineering Systems (pp. 144–148). CRC Press.
[6] Dhabliya, D. (2021c). Designing a Routing Protocol towards Enhancing System Network Lifetime. In Intelligent and Reliable Engineering Systems (pp. 160–163). CRC Press.
[7] Sharma V.R., 'Testing of paraboloidal concentrating solar thermal collector', M.Tech. Dissertation, Energy Systems Engineering, IIT-Bombay, 2005
[8] C.A. Kinjavadekar,V.P.Muley, 'A Test Procedure for Determining Optical Characteristics of a Dish Concentrator and its Implementation on a Scheffler Dish', SESI journal, Vol 20, Dec 2010.
[9] Patwardhan et al., 'Solar central receiver system employing common positioning mechanism for heliostats', United States Patent Application, Jan 2011.
[10] Clifford K. Ho, Siri S. Khalsa, 'A flux mapping method for central receiver systems', Proceedings of the ASME 2011, August 7-10, 2011.
[11] Alberto Sanchez-Gonzalez, Domingo Santana, 'Solar flux distribution on central receivers: A projection method from analytic function', Renewable energy 74, 576 – 587 (2014).
[12] Solar Energy: Principle of Thermal Collection and Storage, S. P. Sukhatme, Tata McGraw Hill production
[13] Ashish R. Pawar, "Roof Crash Simulation of Passenger Car for Improving Occupant Safety in Cabin" in Elsevier Journal
[14] Ashish R. Pawar, "Design and Development: A Simulation Approach of Multi-Link Front Suspension for an All-Terrain Vehicle", SAE Technical Paper, SIAT 2021
[15] Aditya Pawar, Aniket Wanjale, Harshal Wanjale, Yash Sathe, Ashish R. Pawar, "Static Structural Analysis & Optimization Of Driver Cabin Mounting Bracket Of Heavy Commercial Vehicle", Journal of Analysis & Computation (IJAC, UGC), Volume XV Issue VI, June 2021 ISSN: 0973-2861, pp. 111-124
[16] Siddharth P. Patil, Saurabh R. Birwatkar, Pranil D. Phadke, Karan R. Pawar, Ashish R. Pawar, "Static Structural Analysis & Topology Optimization Of Automotive Track Control

Arm For Light Passenger Vehicle", Journal of Analysis & Computation (IJAC, UGC), Volume XV Issue VI, June 2021 ISSN: 0973-2861, pp. 91-100

[17] Sandhya R. More, Ganesh E. Kondalkar, Ashish R. Pawar, "Crash Analysis Of A Conformable CNG Tank Using FEA Tool", Journal of Analysis & Computation (IJAC, UGC), Volume XV Issue VI, June 2021 ISSN: 0973-2861, pp. 71-78

[18] Sumit Ekbote, Sidhhesh Gade, Sanket Mhetre, Raj Dhawade, Ashish R. Pawar, "Experimental Analysis Of Automatically Manufactured Chain Link Fencing Wire", Journal of Analysis & Computation (IJAC, UGC), Volume XV Issue VI, June 2021 ISSN: 0973- 2861, pp. 57-67

[19] Tushar S. Kalaskar, Kashinath H. Munde, Ashish R. Pawar, "Design And Analysis Of Hybrid Aluminium-Composite Driveshaft With Crack Using Experimental Modal Analysis And FEA", Journal of Analysis & Computation (IJAC, UGC), Volume XV Issue VI, June 2021 ISSN: 0973-2861, pp. 27-40

[20] Sandhya R. More, Ganesh E. Kondalkar, Ashish R. Pawar, "Review Of Conformable Cng Tank Storage In Light Goods Vehicle", Journal of Analysis & Computation (IJAC, UGC), Volume XV Issue VI, June 2021 ISSN: 0973-2861, pp. 21-26

[21] Deepak N. Patil, Ganesh E. Kondhalkar, Ashish R. Pawar, "Improvement In Productivity And Quality Of Bumper Punching Machine", Journal of Analysis & Computation (IJAC, UGC), Volume XV Issue V, May 2021 ISSN: 0973-2861, pp. 1-6

[22] Shubham A. Andore, Ashish R. Pawar, P. N. Abhyankar, "Study Of Effects Of Different Profiles Of Dental Implant Using FEA", Journal of Analysis & Computation (IJAC, UGC), Volume XV Issue V, May 2021 ISSN: 0973-2861, pp. 1-13

[23] Abhilash D. Bhosale, Ashish R. Pawar, "Experimental & Numerical Investigation Of Pretention Effect On Fatigue Life Of Double Lap Bolted Joint Under Dynamic Shear Loading", Journal of Analysis & Computation (IJAC, UGC), Volume XV Issue V, May 2021 ISSN: 0973-2861, pp. 1-19

[24] Deepak N. Patil, Ganesh E. Kondhalkar, Ashish R. Pawar, "Structural Optimization Of Bumperfog Lamp Punching Machine", Journal of Analysis & Computation (IJAC, UGC), Volume XV Issue V, May 2021 ISSN: 0973-2861, pp. 71-84

[25] Ashish Pawar, Suraj Jadhav, "Investigate Optimum Shape of Crash Box Analysis Experimentally & Numerically on Geometry Aspect" in Journal of Analysis & Computation (IJAC, UGC), Volume XIV Issue VII, July 2020 ISSN: 0973-2861

[26] Ashish Pawar, Yogesh Vyavahare, Ganesh Kondhalkar, "Roof Crash Simulation of Passenger Car for Improving Occupant Safety in Cabin" in IUP Journal of Mechanical Engineering, Volume 13 Issue 2/3.

[27] Ashish Pawar, Suraj Jadhav, "Experimental & Non-Linear Analysis to Investigate Optimum Shape Crash Box" in Journal of Interdisciplinary Cycle Research (JICR, UGC), Volume XII Issue VII, July 2020 ISSN: 0022-1945, pp. 966-973

[28] Ashish Pawar, Swastik Kumar Pati, Ganesh Kondhalkar, "Comparative Analysis of Kenaf & Jute E Glass Epoxy Specimen Along with B Pillar Natural & Synthetic Combination Replica Test Under UTM" in Journal of Analysis & Computation (IJAC, UGC), Volume XIV Issue VII, July 2020 ISSN: 0973-2861

[29] Ashish Pawar, Harshal Dharmale, Ganesh Kondhalkar, “Experimental FEA Investigation of Bolt Loosening in a Bolted Joint Structure ” in Journal of Analysis & Computation (IJAC, UGC), Volume XIV Issue VII, July 2020 ISSN: 0973-2861, pp. 1-12

[30] Ashish Pawar, Harshal Dharmale, Ganesh Kondhalkar, “Numerical Investigation Of Bolt Loosening In A Bolted Joint Structure” in Journal of Analysis & Computation (IJAC, UGC), Volume XIV Issue VII, July 2020 ISSN: 0973-2861, pp. 1-12

[31] Ashish Pawar, Abhijeet Salunkhe, Kashinath Munde, “Optimization of Power Lift Gate Spindle & Socket Assembly” in Journal of Analysis & Computation (IJAC, UGC), Volume XIV Issue VII, July 2020 ISSN: 0973-2861

[32] Ashish Pawar, Abhijeet Salunkhe, Kashinath Munde, “Investigate Numerical Analysis of Power Lift Gate Spindle & Socket Assembly with Modifications” in Journal of Analysis & Computation (IJAC, UGC), Volume XIV Issue VII, July 2020 ISSN: 0973-2861

[33] Ashish Pawar, Balasaheb Takale, “ ” in Journal of Analysis & Computation (IJAC, UGC), Volume XIV Issue VII, July 2020 ISSN: 0973-2861

[34] Ashish Pawar, Sampada Ahirrao, Ganesh Kondhalkar, “Fatigue Analysis of Leaf Spring Bracket for Light Duty Vehicles on Topology Optimization Approach” in Journalof Analysis & Computation (IJAC, UGC), Volume XIV Issue VII, July 2020 ISSN: 0973-2861, pp. 1-11

[35] Ashish Pawar, Rahul Nimbalkar, “Investigation of Carbon Fiber & E Glass Epoxy Composite with Multi-Bolt Joints using Tensile Loading ” in Journal of Analysis & Computation (IJAC, UGC), Volume XIV Issue VII, July 2020 ISSN: 0973-2861

[36] Ashish Pawar, Rahul Nimbalkar, “Numerical Analysis of Carbon Fiber & E Glass Epoxy Composite Plates in Tensile Loading with Multi-Bolt Joints” in Journal of Analysis & Computation (IJAC, UGC), Volume XIV Issue VII, July 2020 ISSN: 0973-2861

[37] Ashish Pawar, Makarand Patil, Ganesh Kondhalkar, “Predication of Effect of Welding Process Parameter of MIG Process on Weld Bead Geometry” in Journal of Analysis & Computation (IJAC, UGC), Volume XIV Issue VII, July 2020 ISSN: 0973-2861

[38] Ashish Pawar, “Topology Optimization Of Leaf Spring Bracket For Light Duty Vehicle” in Journal of Emerging Technologies and Innovative Research (JETIR, UGC), Volume 6 Issue 5, May 2019 ISSN: 2349-5162

[39] Ashish R. Pawar, Dr. K. H. Munde, Vidya Wagh, “Stress Analysis of Crane Hook with Different Cross Section Using Finite Element Method” in Journal of Emerging Technologies and Innovative Research (JETIR, UGC), Volume 6 Issue 1, Jan 2019 ISSN: 2349-5162, pp. 79-83

[40] Ashish R. Pawar, Dr. K. H. Munde, Mahesh Mestry, “Pre-Stressed Modal Analysis of Composite Bolted Structure” in Journal of Emerging Technologies and Innovative Research (JETIR, UGC), Volume 5 Issue 7, July 2018 ISSN: 2349-5162

[41] Ashish R. Pawar, Kashinath Munde, Vijay Kalantre, “Topology Optimization of Driver Cabin Mounting Bracket of Heavy Commercial Vehicle” in International Journal of Science & Engineering Development Research (IJSDR), Volume 3, Issue 7, July 2018 ISSN: 2455-2631

[42] Ashish R. Pawar, Kashinath Munde, Vijay Kalantre, “Topology Optimization of Front Leaf Spring Mounting Bracket” in International Journal of Science & Engineering Development Research (IJSDR), Volume 3, Issue 7, July 2018 ISSN: 2455-2631